Contract No:

This document was prepared in conjunction with work accomplished under Contract No. 89303321CEM000080 with the U.S. Department of Energy (DOE) Office of Environmental Management (EM).

Disclaimer:

Determining Migration of Vapor Corrosion Inhibitors Using Corrosion Potential Data

Pavan K. Shukla, Roderick E. Fuentes, and Bruce J. Wiersma
Savannah River National Laboratory®
Aiken, South Carolina, 29808
USA

Crystal Girardot, Jason Page, and Shawn Campbell
Washington River Protection Solutions
2425 Stevens Center Pl
Richland, Washington, 99352
USA

ABSTRACT

Hanford stores millions of gallons of high-level waste in 27 carbon-steel double shell, underground tanks. A secondary shell surrounds the primary shell, where the bottom plate of the secondary shell rests on a channeled concrete pad. There have been instances of metal loss on the secondary shell bottom plates in contact with the concrete basemat where groundwater accumulation in the channels may have caused corrosion. In addition, uneven contact between the basemat and shell could create occluded areas where localized corrosion is possible. In previous studies, vapor corrosion inhibitors (VCIs) were tested for their ability to mitigate concrete-basemat side corrosion of the secondary shell bottom. The previous study indicated that VCIs are effective in mitigating corrosion in both immersed and vapor space conditions. However, the tanks being large with approximately 70-ft bottom, it is important to understand VCI distribution rate after VCIs are injected. It was determined that corrosion potential is a good indicator of VCI concentration in the simulated groundwater solution. Experiments were conducted with VCI injection in the groundwater along with coupons positioned at several locations with respect to the ground water. Coupons' potentials were monitored, and corrosion rate data were analyzed. The paper presents result and analysis of the experimental data.

Key words: Vapor Corrosion Inhibitors, Hanford, Double Shell Tanks, Bottom Plate, Pitting Corrosion.

INTRODUCTION

High-level radioactive waste generated during reprocessing of spent nuclear fuel at Hanford has been stored in several single- and 27 double shell tanks (DSTs). Each DST consists of a primary shell (inner) surrounded by secondary (outer) liner. The secondary liner rests on a concrete foundation. Rainwater seeps in and accumulates in the drain slots and may corrode the exterior of the secondary liner. Evidence of wall thinning has been detected via ultrasonic inspections of the annulus floor between the primary and secondary tank shells. Since the inspection is confined to this region, there is a concern that corrosion is widespread on the underside of the bottom plate. Since the rainwater level can vary in the drain slots based on accumulation, corrosion could be caused by direct contact with the accumulated water; when the leak detection pit (LDP) water level is below the structural limit, vapor space corrosion (VSC) could also occur. Accumulated water is drained through the sumps in the LDP. The LDP water

was analyzed for its constituents, and two simulants were developed considering the chemical composition range of the accumulated water. The simulants are identified as leak detection pit and ground water (GW); compositions are listed in Table 1. A previous study established that GW simulant is more corrosive than the leak detection pit, therefore GW was used in the VCI effectiveness study.[1]

Laboratory experiments were conducted to address the concerns of both immersed-phase corrosion and VSC of the tank steel exposed to GW simulant. VCIs were also tested to determine their efficacy in mitigating the corrosion on pre-corroded surfaces. VCIs' application for above ground storage tank bottom corrosion control is recent, and several studies have documented effectiveness of VCIs for tank bottom plate corrosion control.[2,3,4] One of the key questions regarding VCIs' delivery is their migration rates. A previous study with VCI focused on tank bottom application has indicated that corrosion potential values provide an indication of the migration of the VCIs.[4] This study was focused on understanding the coupons' corrosion potentials in immersed and vapor space coupons as a function of VCI concentration.

Table 1
Composition of the Leak Detection Pit and Ground Water Simulants

Source chemical	Concentration (M)	
	Leak Detection Pit	Ground Water
Sodium bicarbonate	1.12×10^{-3}	1.75×10^{-3}
Calcium hydroxide	1.21×10^{-4}	1.50×10^{-3}
Potassium nitrate	6.75×10^{-5}	2.40×10^{-4}
Magnesium Nitrate, 6hydrate	1.52×10^{-5}	–
Strontium Nitrate	4.04×10^{-6}	2.87×10^{-6}
Sodium sulfate	1.83×10^{-6}	–
Ferric sulfate	–	6.25×10^{-4}
Sodium Metasilicate, 5hydrate	4.57×10^{-5}	6.00×10^{-4}
Ferric chloride	2.67×10^{-6}	7.67×10^{-5}7E-05
Manganese Chloride	–	3.100E-04
Acetic Acid	3.00×10^{-4}	3.000E-04
Adjusted pH	7.6	7.6

EXPERIMENTAL

Several experiments were set up using GW simulant as electrolyte. The first experiment was a control experiment, and no VCI was added to this experiment, and the coupons were not monitored for their corrosion potentials. A second test was conducted with a commercially available VCI, and recommended dosage of the VCI was used. The VCI was added to the GW simulant at the start of the test. The coupons in the second test were monitored for their corrosion potential. A third test was conducted in parallel to the second test. In this test, the coupons were immersed in the GW simulant only with no VCI, and coupons corrosion potentials were monitored.

Disk coupons, machined from a legacy carbon steel plate, were used in the experiments. The legacy carbon steel is based on specifications of Association of American Railroads(1) Tank Car (AAR TC 128) steel, and its chemistry and microstructure are similar to the vintage steel from which the tanks were fabricated UNS K02401 (i.e., American Society for Testing and Materials (ASTM)(2) A515 Grade 60 carbon steel). The chemical composition of the legacy carbon steel is listed in Table 2. All elemental compositions except for Mn and Si meet the ASTM A515 Grade 60 specification. The coupons were 25 mm (1 inch) diameter with a thickness of 3 mm (0.125 inch) and polished to a 600-grit finish. The coupons

(1) American Association of Railroads, 425 3rd Street SW, Washington, DC 20024
(2) ASTM International, 100 Barr Harbor Dr., West Conshohocken, PA 19428-2959

were potted in a mold prepared with a two-part transparent epoxy mold, such that that one face of the coupon was exposed to the test electrolyte. The coupons' exposed surfaces were modified to simulate crevice corrosion. A crevice former was attached to each coupon surface using tape and wire. The crevice formers partially covered coupons' surfaces, which created conditions for localized corrosion under the crevice formers. An image of the coupon with the crevice former is presented in Figure 1; these coupons were used in the first experiment. For the second and third experiments, the coupons with the crevice former were slightly modified. A platinum (Pt) wire was added to the coupon assembly as shown in Figure 2. The Pt-wire was connected to the metal surface through an interconnecting Nafion™ film which was cured as per the procedure detain in Hsu and Wan[5] before using it to connect the Pt wire with the metal surface. The use of Pt wire was needed to ensure electrical continuity between the coupon surface and Pt wire on each coupon assembly, especially needed for the vapor phase coupons to be able to measure coupons' metal surface potential with respect to the Pt-wires. Additional experimental details are in Shukla et al.[6]

Table 2
Chemical Composition of AAR TC 128 Steel (wt.%)

	C	Mn	P	S	Si	Fe
Specification	0.24 (max.)	0.9 (max.)	0.035 (max.)	0.04 (max.)	0.13 to 0.33	Balance
Measured	0.212	1.029	0.012	0.013	0.061	Balance

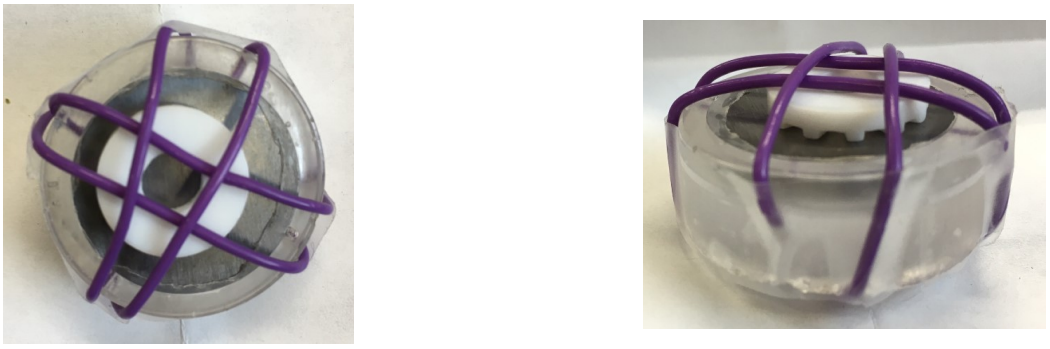

(a) Top view **(b) Side View**

Figure 1. (a) Top, and (b) Side views of the partially covered coupon. The coupon's surface is partially covered with a crevice former, which is held in place using purple wire and tape

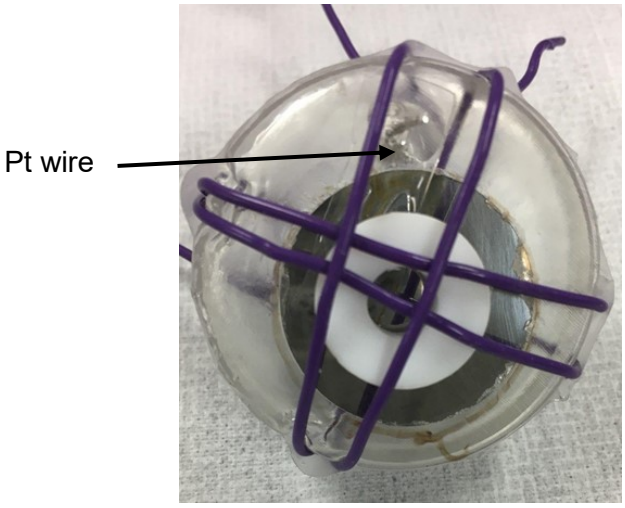

Figure 2. Top view of the partially covered coupon with platinum wire and Nafion™ film interconnecting the Pt-wire with the metal surface.

A glass vessel of dimensions 1.0 m (3.3 ft) tall and 14 cm (5.5 inch) diameter was used for each experiment. Approximately 1.25 L of GW simulant was added to a vessel for each experiment. Each vessel has a water jacket around the simulant holding area which was used to circulate warm water to maintain the simulant temperature at 45 ± 2 °C. Each vessel also has several ports, which were used to insert thermocouples and electrical resistance (ER) probes. An image showing the three vessels used is presented in Figure 3. Coupons were exposed to the electrolyte and vapors of the electrolyte in each experiment by suspending them using rods. The coupons were suspended such that the exposed surfaces of the vapor space coupons were facing the electrolyte. The rods holding the coupons were placed inside the vessels. Several coupons were immersed in each vessel, and coupons were also placed in vapor space of each vessel. The vapor space coupons were placed at several height levels with respect to the electrolyte using the rods. The coupons' positions, with respect to electrolyte in each vessel, simulated different vapor space conditions and water levels in the drain slots. These levels, representing the drain slot characteristics and its position with respect to the bottom, are described:

Level 1: Bottom or low level. Coupons were dipped in the simulant for five minutes prior to testing. The coupons were hung at the bottom fixed ring of the rod. These coupons were suspended approximately 25 mm (1 inch) above the liquid level of the simulant. Every two weeks, the coupons were lowered into the simulant for 5 minutes. This level is representative of the situation when the secondary liner bottom plate experienced periodic wetting/drying.

Level 2: Intermediate or middle level. Coupons were dipped in the simulant for five minutes prior to testing. The coupons were hung at the middle-fixed ring approximately 46 cm (18 inch) above the liquid simulant in each vessel. This level is representative of a vapor space region of the secondary liner bottom that at one time was exposed to water but has infrequent or no contact with the water. However, this region is exposed to the humidified air.

Level 3: Top or high level. This set of coupons was not exposed to the solution prior to testing. The coupons were suspended approximately 92 cm (36 inch) above the simulant. This level is representative of the secondary liner bottom plate region that is only exposed to the humidified air and any volatile species from the solution.

A description of the vessels for each electrolyte is provided in Table 3. Electrical Resistance (ER) probes were placed in Vessels 1, 2, and 3; placement positions are detailed in Table 3. ER probe data were collected periodically. Coupons were removed after several months of exposure, cleaned with Clarke's solution[7] to remove corrosion products, and weighed to determine the mass loss of each coupon.

Table 3
Electrolyte Description, Vessel Identification, and Coupons and ER Probe Information

Electrolyte	Corrosion Cell	Notes
GW simulant only, exposure time of six months	Vessel 1	• 6 coupons each in immersed, Level 1, Level 2, and Level 3 positions, total 24 coupons. • ER probes at each level. Cylindrical element probes at immersed, Levels 1 and 3, and wire element probe at Level 3.
GW simulant mixed with the VCI as per the VCI-vendor recommended concentration	Vessel 2	• 6 coupons each in immersed, Level 1, Level 2, and Level 3 positions, total 24 coupons. • Each coupon had Pt-wire in its assembly; vapor space coupons' potentials were measured with respect the P-wire. The immersed phase coupons'

Table 3
Electrolyte Description, Vessel Identification, and Coupons and ER Probe Information

Electrolyte	Corrosion Cell	Notes
		potentials were measured with respect to the Pt-wires and also with respect to saturated calomel reference electrode.
GW simulant only, exposure time of six months	Vessel 3	• 2 coupons in immersed in the electrolyte. • Both coupons had Pt-wire in their assemblies. Coupons' potentials were measured with respect to the Pt wires and also with respect to the saturated calomel reference electrode.

Figure 3. Image of the experimental setup.

Pitting and patch-like corrosion occurred on all the coupons. Coupons were cleaned, and each coupon's mass change was also recorded. In addition, coupon surfaces were profiled and the deepest pit in each coupon was measured using the surface profile data.

EXPERIMENTAL DATA AND RESULTS

The mass-loss data for the coupons in Vessel 1 are listed in Table 4; the data is for the coupons exposed to GW simulant only for the six months. The table has averages and standard deviations of the mass-loss data. Several sets of coupons were exposed to GW simulant only for two months. The data listed in Table 4 is presented in Figure 4. As seen in the figure, the coupons continued to corrode even after two months of exposure. In fact, the 6-month coupons at Levels 1 and 3 corroded at faster rate than the 2-month coupons. This indicated that a mitigation strategy is necessary and VCIs are one option.

Table 4
Mass Loss Data of Coupons Exposed to GW Simulant for Two and Six Months

Level	Coupon Mass Loss (mg)	
	2-month Exposure**	6-month Exposure**
Immersed	90.7 ± 12.5	155.7 ± 17.0
Level 1	44.3 ± 26.3	130.3 ± 20.7
Level 2	57.7 ± 18.9	87.6 ± 13.6
Level 3	35.3 ± 13.8	126.9 ± 38.0
**2- and 6-month coupons were exposed to GW only, each data point for 2-month corrosion rate represent average of 12 coupons and each data point for 6-month coupon represent average of six coupons		

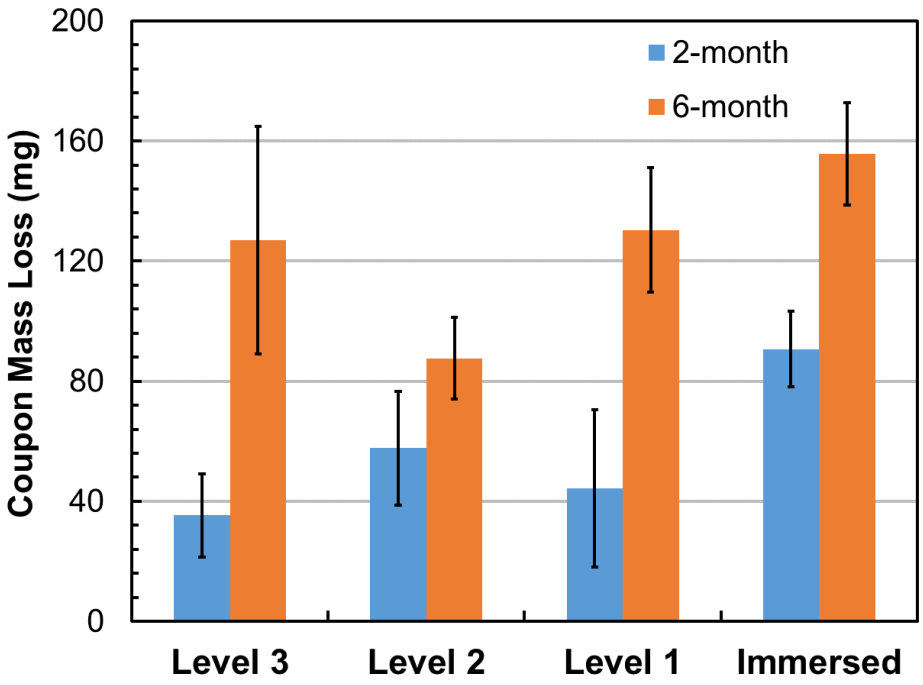

Figure 4. Two- and six-month coupons mass loss data. The coupons were exposed to the ground water simulant.

The corrosion potentials of the coupons in Vessels 2 and 3 were monitored periodically. The coupons were identified using a numerical value. The coupons identification numbers are listed in Table 5. The corrosion potentials of the coupons in immersed phase were measured with respect to the SCE and Pt-wire. The corrosion potential data for the coupons and Pt wires in Vessels 2 and 3 are presented in Figure 5.

The corrosion potentials of the vapor space coupons could only be measured with the respect to the Pt wire embedded in each coupon assembly. The potential data for the coupons in Vessel 2 at Levels 1, 2, and 3 are presented in Figures 6(a), 6(b), and 6(c), respectively.

Table 5
Coupons Position and Identification Number in the GW plus VCI and GW only Experiments

Level	GW plus VCI Experiment in Vessel 2	GW Only Experiment in Vessel 3
Immersed	34, 35, 36	37, 38
Level 1	31, 32, 33	—
Level 2	28, 29, 30	—
Level 3	25, 26, 27	—

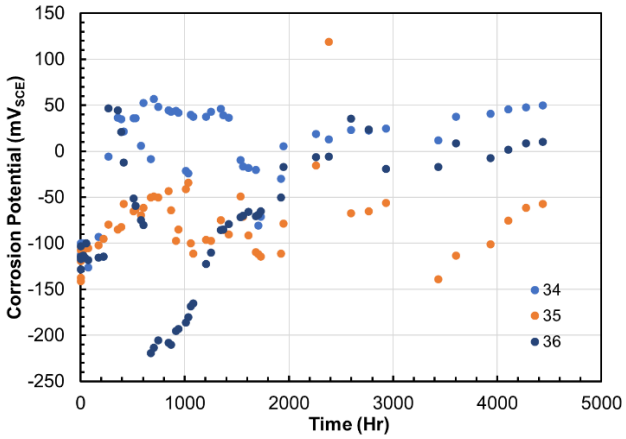

(a) Immersed coupons in GW + VCI with respect to SCE

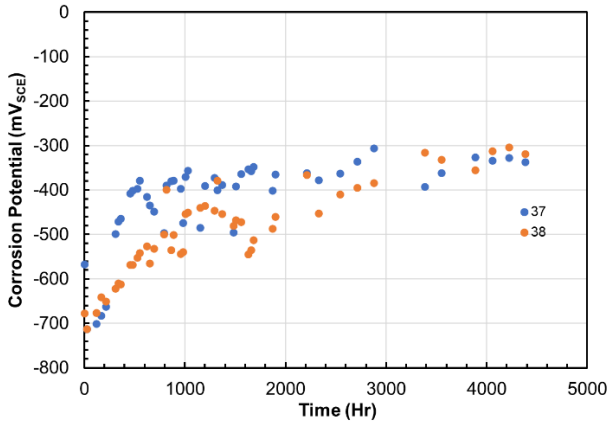

(b) Immersed coupons in GW only with respect to SCE

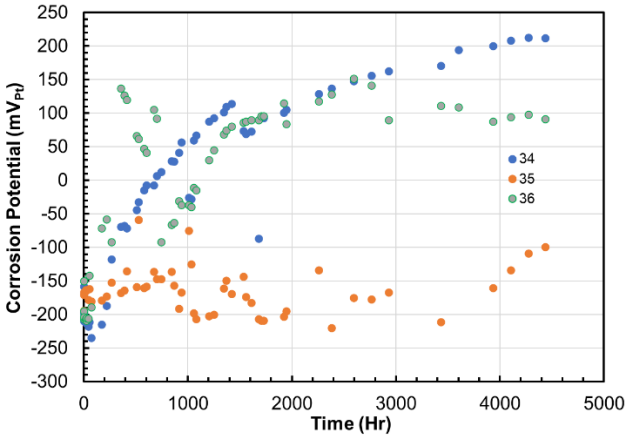

(c) Immersed Pt-wire in GW + VCI with respect to SCE

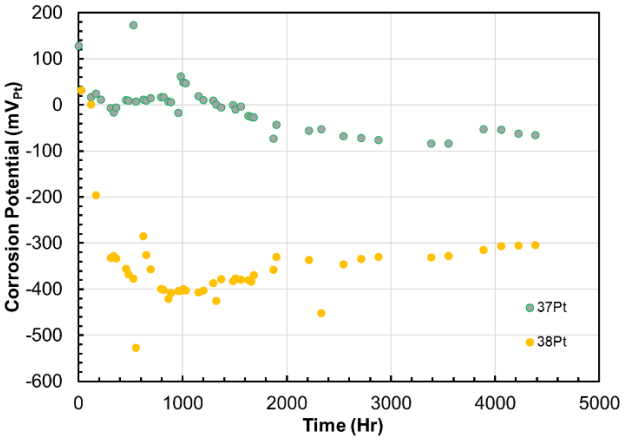

(d) Immersed Pt-wire in GW only with respect to SCE

Figure 5. Corrosion potentials of the immersed coupons and Pt-wires with respect to saturated calomel reference electrode.

The corrosion potential data are summarized in Table 6. The corrosion potentials of the immersed coupons in GW are close to -325 mV_{SCE}, and in GW + VCI were in the range of -50 to +50 mV_{SCE}. This indicated that corrosion potential difference is close to 300 mV between the GW and GW + VCI solutions. The corrosion potentials of the Pt wire in GW immersed solution are -300 and -50 mV_{SCE}, and in

GW + VCI range between -100 to 200 mV_{SCE}; Pt wire potentials were not distinctly different and overlapped. A comparison between the SCE-measured and Pt-wire measured potentials indicated that Pt wire potentials are not stable, and a stable difference in the Pt wire potentials between the two solutions (GW + VCI and GW) was not established.

Regarding the vapor space coupons in Vessel 2, of the three coupons at Level 1, the corrosion potentials of the two coupons are close of 0 mV_{Pt} whereas potential of the third coupon is close to -300 mV_{Pt} after six months of exposure. Similarly, the corrosion potentials of the three Level 2 coupons with respect to Pt wires are in the range of -228 to -164 mV_{Pt}, and corrosion potentials of the Level 3 coupons are in range of -212 to -182 mV_{Pt}. The corrosion potential data of the coupons with respect to the Pt wires indicate that the Pt-referenced corrosion potentials were not stable in vapor phase.

The coupons were extracted after six months of exposure in Vessels 2 and 3. Images of the coupons extracted from Vessel 2 are presented in Figure 7. The coupons were cleaned and processed. The coupons corrosion rate data are listed in Table 7. Each coupon's surface was profiled. The profiled images of the coupons are presented in Figure 8. Each coupon's surface average and pitting corrosion rate data are listed in Table 7 and are graphically presented in Figure 9.

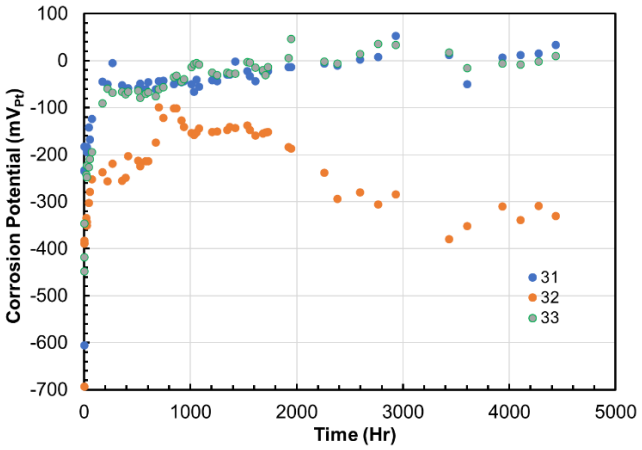

(a) Level 1 coupons in GW + VCI with respect to Pt-wire

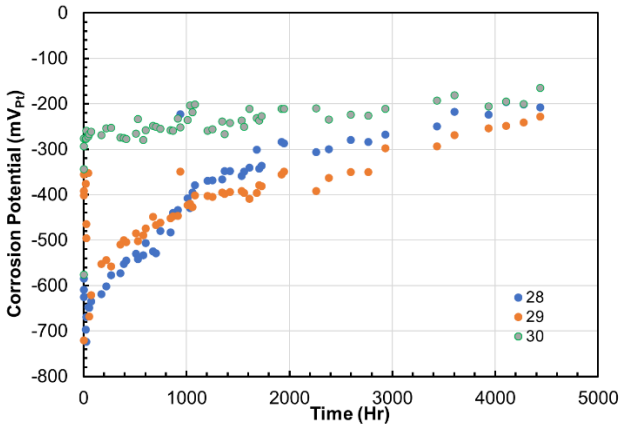

(b) Level 2 coupons in GW + VCI with respect to Pt-wire

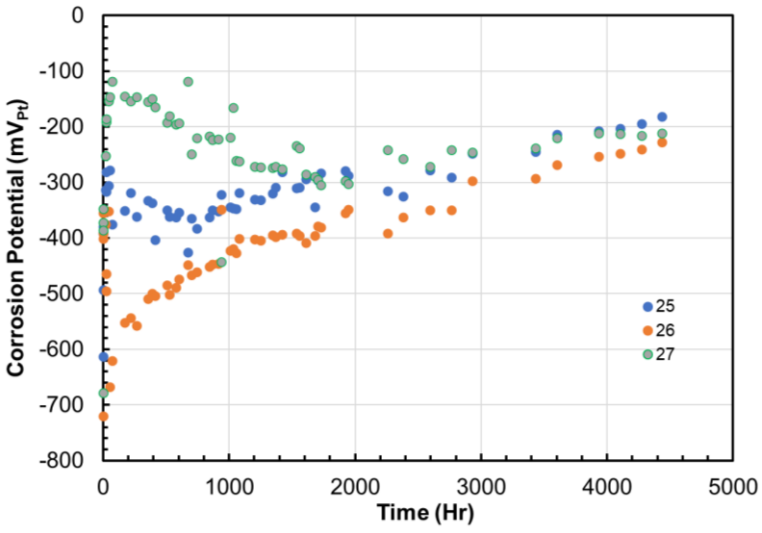

(c) Level 3 coupons in GW + VCI with respect to Pt-wire

Figure 6. Corrosion potentials of the Levels 1, 2, and 3 coupons with respect to Pt-wires.

Table 6
Immersed Pt Wire and Coupons Potentials

Coupons/Pt Wire	Electrolyte	
	GW only	GW + VCI
Pt wire (with immersed coupons) vs. SCE	Coupon 37 wire near -300 mV Coupon 38 wire near -50 mV	Coupons 34 and 36 wires near 200 and 100 mV, respectively Coupon 35 wire near 100 mV
Immersed Coupons vs. SCE	Two coupons near -325 mV	Three coupons' potentials within ±50 mV
Level 1 Coupons vs. Pt wire	—	Two coupons near 0 mV, third coupon at -300 mV
Level 2 Coupons vs. Pt wire	—	Coupons' potentials range between --228 to -164 mV
Level 3 Coupons vs. Pt wire	—	Coupons' potentials range between --212 to -182 mV

Table 7
Corrosion Rates of the Coupons Exposed to GW + VCI Solution in Vessel 2

Level	Corrosion Type	Corrosion Rate (mpy)			Average + Std of Surface Average Corrosion Rate (mpy)	Average + Std of Pitting Corrosion Rate (mpy)
		Coupon 1	Coupon 2	Coupon 3		
Level 3	Surface Average	1.47	2.88	0.37	1.57 ± 1.26	33.3 ± 21.7
	Pitting Corrosion	50.8	40.1	9.0		
Level 2	Surface Average	3.11	3.64	0.68	2.48 ± 1.58	44.5 ± 19.5
	Pitting Corrosion	60.5	50.2	22.7		
Level 1	Surface Average	0.82	0.32	0.16	0.34 ± 0.34	8.0 ± 0.7
	Pitting Corrosion	8.7	7.8	7.4		
Immersed	Surface Average	0.19	0.14	0.19	0.17 ± 0.03	1.2 ± 0.2
	Pitting Corrosion	1.3	1.4	1.0		

Examination of the profiled images of the coupons showed that deep pits occurred on most of the coupons where Nafion film was used to electrically connect the Pt wire and metal surface in each coupon assembly.

Images of the coupons retrieved from Vessel 3 after six months of exposure to GW simulant are presented in Figure 10. The profiled images of the coupons, obtained after cleaning the corrosion products, are also presented in Figure 10. The coupons in Figure 10 were profiled using the same color

map scale as in Figure 8. Both Vessel 3 coupons were immersed in GW, but only Coupon 38 had Nafion to interconnect Pt wire and coupon surface. As seen in Figure 10, the coupon with Nafion has more concentrated corrosion, directly underneath the Nafion film coverage. The corrosion rate data for the two coupons in Vessel 3 is summarized in Table 8. The Nafion film pieces were visually examined after the test. It was found that the Nafion film pieces have become more brittle after the tests. This indicated that both physical and chemical properties of Nafion degraded during the GW and GW + VCI exposure tests.

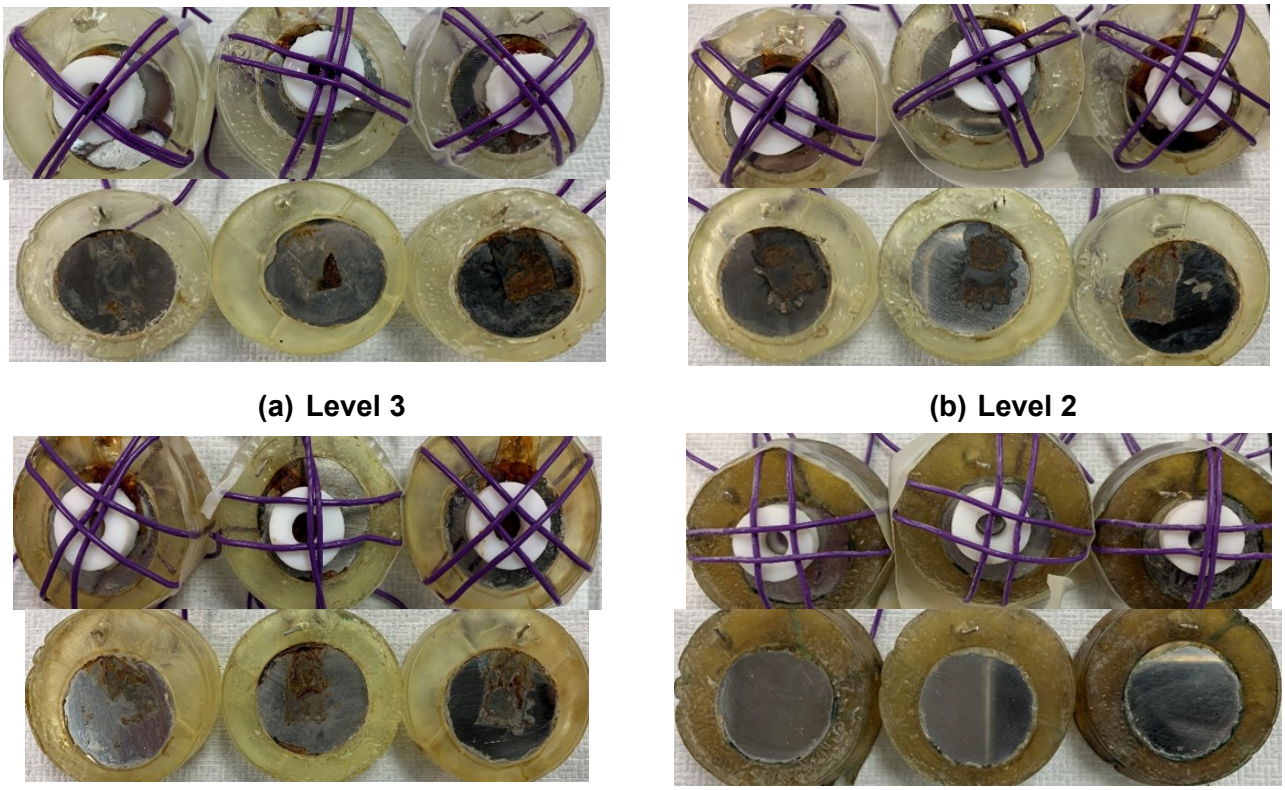

(a) Level 3 **(b) Level 2**

(c) Level 1 **(a) Immersed**

Figure 7. Post-test images of the coupons exposed to GW + VCI in Vessel 2

Table 8
Corrosion Rates of the Coupons Exposed to GW Solution in Vessel 3

Coupon Number	Condition	Corrosion Rate
37	Immersed, No Nafion	Surface average corrosion Rate: 8.1 mpy Pitting corrosion rate: 36.4 mpy
38	Immersed, Nafion to connect PT wire and coupon surface	Surface average corrosion rate: 7.9 mpy Pitting Corrosion Rate: 30.9 mpy

Both post-test examination of the coupons and corrosion potential data indicated that corrosion potentials were not stable with respect to Pt wires, and steady-state potentials could not be measured. Pos-test examination of Nafion film pieces indicated that the film pieces physically and chemically altered during the experiments; this may have resulted in unsteady potentials of the Pt wires, and hence, unsteady potentials of the coupons with respect to the Pt wires.

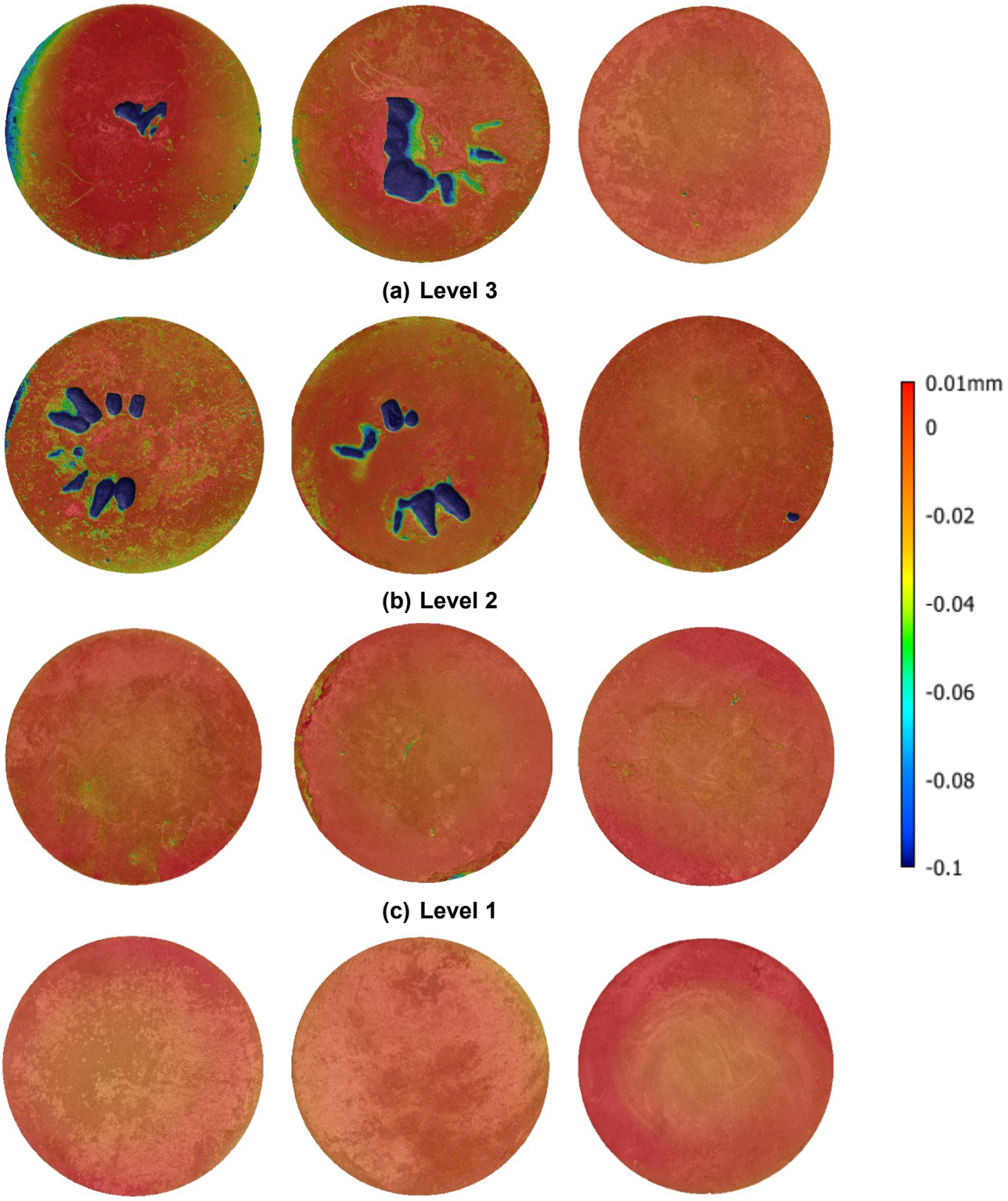

(a) Level 3

(b) Level 2

(c) Level 1

(d) Immersed

Figure 8. Post-test profiled images of the coupons exposed to GW + VCI in Vessel 2

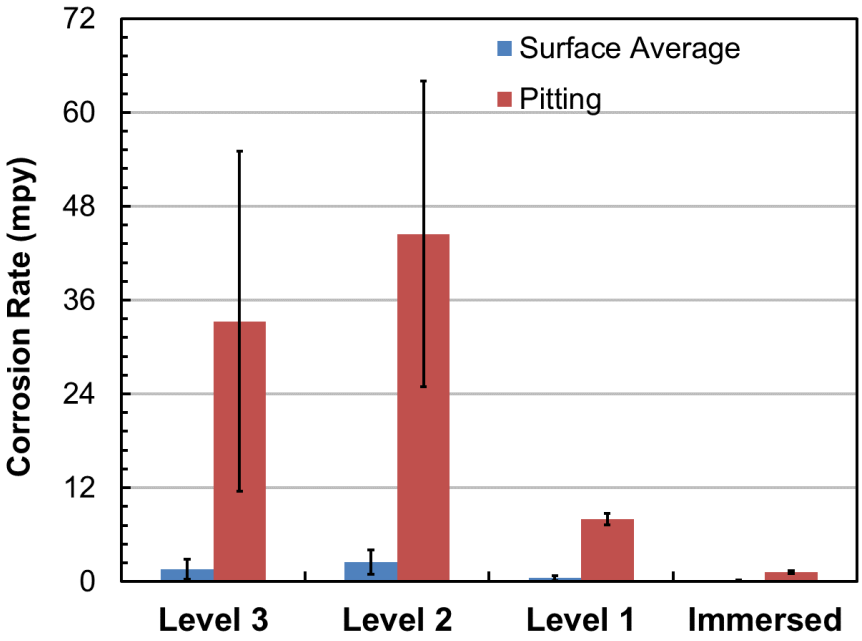

Figure 9. Corrosion rate data of the coupons exposed to GW + VCI in Vessel 2

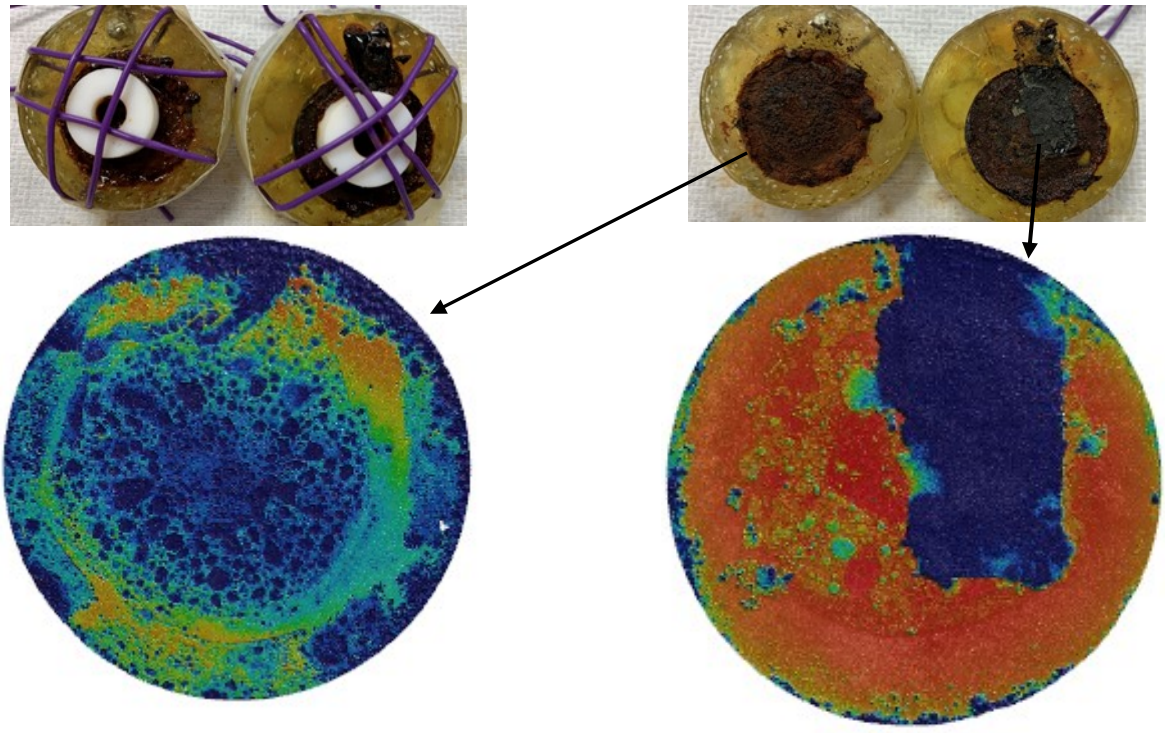

Coupon 37 **Coupon 38**

Figure 10. Post-test images and profiled images of the coupons exposed to GW in Vessel 3

CONCLUSION

The two- and six-month coupon data indicated that aggressive corrosion continues even after first two months of exposure to GW simulant. This indicated the need to use corrosion mitigation methods such as VCIs for the secondary liners at the Hanford site. However, determining migration rates of the VCIs is critical to field implementation of the VCI technology. It was hypothesized that corrosion potential data can be used to study and determine migration of VCIs. A Pt-wire embedded in each coupon assembly was used as reference for the vapor space and immersed phase coupons in GW + VCI and GW only electrolytes. Saturated calomel electrode was also used as reference for the immersed coupons. The immersed coupons' corrosion potentials in GW + VCI electrolyte were distinctly different compared to GW only electrolyte, when measured with respect to the saturated calomel electrode. However, the corrosion potentials of the immersed Pt wires in the two electrolytes overlapped, indicating that Pt wires' potentials were not steady, and Pt wires could not be used as references to measure corrosion potentials of the coupons. This study indicated that corrosion potentials could be used to study and determine migration of the VCIs, however, a steady reference electrode is needed to measure the corrosion potentials accurately.

ACKNOWLEDGEMENT

This work was produced by Battelle Savannah River Alliance, LLC under Contract No. 89303321CEM000080 with the U.S. Department of Energy. Publisher acknowledges the U.S. Government license to provide public access under the DOE Public Access Plan (http://energy.gov/downloads/doe-public-access-plan)."

REFERENCES

1. R. E. Fuentes, P. K. Shukla, B. J. Wiersma, C. Girardot, N. Young and T. Venetz, "Effects of Vapor Corrosion Inhibitors on Corrosion of Secondary Liner in Double Shell Tanks at Hanford," CORROSION/2019, Paper No. C2019-13369 (Houston, TX, NACE, 2019).

2. E. Lyublinski, G. Ramdas, Y. Vaks, T. Natale, M. Posner, K. Baker, R. Singh, and M. Schultz. "Corrosion Protection of Soil Side Bottoms of Aboveground Storage Tanks." CORROSION/2014, Paper No. 4337 (Houston, TX, NACE, 2014).

3. P. Shukla, R. E. Fuentes, B. J. Wiersma, C. Girardot, N. Young, and T. Venetz, "Performance of Vapor Corrosion Inhibitors on Mitigating Corrosion of Secondary Liner in Double Shell Storage Tanks at Hanford," CORROSION/2020, Paper No. C2020-14846 (Houston, TX, NACE, 2020).

4. P. Shukla, X. He, O. Pensado, A. Nordquist, "Vapor Corrosion Inhibitors Effectiveness for Tank Bottom Plate Corrosion Control," Report Catalog Number PR–015–153602-R01 (Chantilly, VA: PRCI, Inc. 2018).

5. C.H. Hsu, C.C. Wan, "An Innovative Process for PEMFC Electrodes Using the Expansion of Nafion Film," Journal of Power Sources, Vol. 115, pp. 268–273, 2003.

6. P. Shukla, R. E. Fuentes, B. J. Wiersma, C. Girardot, J. Page, "Performance of Vapor Corrosion Inhibitors for Localized Corrosion Mitigation of Double Shell Storage Tanks at Hanford," CORROSION/2021, Paper No. C2021-16629 (Houston, TX, NACE, 2021).

7. ASTM International. ASTM G1–03 (Reapproved 2017), "Standard Practice for Preparing, Cleaning, and Evaluating Corrosion Test Specimens." West Conshohocken, Pennsylvania: ASTM International. 2014.